Chronic Diabetes Increases Advanced Glycation End Products on Cardiac Ryanodine Receptors/Calcium-Release Channels

Keshore R. Bidasee,[1] Karuna Nallani,[2] Yongqi Yu,[2] Ross R. Cocklin,[3] Yinong Zhang,[3] Mu Wang,[3] Ü. Deniz Dincer,[4] and Henry R. Besch, Jr.[2,5]

Decrease in cardiac contractility is a hallmark of chronic diabetes. Previously we showed that this defect results, at least in part, from a dysfunction of the type 2 ryanodine receptor calcium-release channel (RyR2). The mechanism(s) underlying RyR2 dysfunction is not fully understood. The present study was designed to determine whether non–cross-linking advanced glycation end products (AGEs) on RyR2 increase with chronic diabetes and if formation of these post-translational complexes could be attenuated with insulin treatment. Overnight digestion of RyR2 from 8-week control animals (8C) with trypsin afforded 298 peptides with monoisotopic mass ($M+H^+$) ≥500. Digestion of RyR2 from 8-week streptozotocin-induced diabetic animals (8D) afforded 21% fewer peptides, whereas RyR2 from 6-week diabetic/2-week insulin-treated animals generated 304 peptides. Using an in-house PERLscript algorithm, search of matrix-assisted laser desorption ionization–time of flight mass data files identified several $M+H^+$ peaks corresponding to theoretical RyR2 peptides with single N^{ϵ}-(carboxymethyl)-lysine, imidazolone A, imidazone B, pyrraline, or 1-alkyl-2-formyl-3,4-glycosyl pyrrole modification that were present in 8D but not 8C. Insulin treatment minimized production of some of these nonenzymatic glycation products. These data show for the first time that AGEs are formed on intracellular RyR2 during diabetes. Because AGE complexes are known to compromise protein activity, these data suggest a potential mechanism for diabetes-induced RyR2 dysfunction. *Diabetes* 52:1825–1836, 2003

From the [1]Department of Pharmacology, University of Nebraska Medical Center, Omaha, Nebraska; the [2]Department of Pharmacology and Toxicology, Indiana University School of Medicine, Indianapolis, Indiana; the [3]Department of Biochemistry and Molecular Biology, Indiana University School of Medicine, Indianapolis, Indiana; the [4]Department of Pharmacology, Faculty of Pharmacy, University of Ankara, Tandogan, Ankara, Turkey; and the [5]Krannert Institute of Cardiology, Center for Vascular Biology and Medicine, Indianapolis, Indiana.

Address correspondence and reprint requests to Keshore R. Bidasee, Department of Pharmacology, University of Nebraska Medical Center, 986260 Nebraska Medical Center, Omaha, NE 68198-6260. E-mail: kbidasee@unmc.edu.

Received for publication 26 January 2003 and accepted in revised form 31 March 2003.

6D-2I, 6-week streptozotocin-induced diabetic/2-week insulin-treated animals; 8C, 8-week control animals; 8D, 8-week streptozotocin-induced diabetic animals; AFGP, 1-alkyl-2-formyl-3,4-glycosyl pyrrole molecule; AGE, advanced glycation end product; K_d, equilibrium dissociation constant; $M+H^+$, monoisotopic mass; MALDI-TOF, matrix-assisted laser desorption ionization–time of flight; RAGE, receptor for AGEs; RyR2, type 2 ryanodine receptor calcium-release channel; STZ, streptozotocin.

A significant percentage of patients with diabetes (both type 1 and type 2) develop a unique cardiomyopathy that is independent of coronary atherosclerosis (1–3). This "diabetic cardiomyopathy" as it is termed starts off with asymptomatic left ventricular diastolic dysfunction (slowing of relaxation kinetics). As the disease progresses, systolic function becomes compromised, leading to an increase in incidence of morbidity and mortality (4–6).

The release of calcium ions from internal sarcoplasmic reticulum via the type 2 ryanodine receptor calcium-release channel (RyR2) is an integral step in the cascade of events leading to cardiac muscle contraction (7). We and others have shown that expression of this protein decreases in hearts of chronic diabetic patients (8,9) as well as in the streptozotocin (STZ)-induced diabetic rats (10–13). Using the latter model, we found that in addition to a decrease in expression of RyR2, its functional integrity is also compromised in diabetes (14,15). This dysfunction is manifested as a decrease in RyR2 ability to bind the specific ligand [^{3}H]ryanodine and a slowing in its electrophoretic mobility using denaturing SDS-PAGE.

Two distinct and separate types of post-translational modifications are likely to be induced by diabetes. First, it is well known that metabolic changes brought about by diabetes increase production of reactive oxygen species (e.g., superoxide anions [$O^{\cdot}$], hydroxy radicals [$OH^{\cdot}$], lipid peroxides [$ROO^{\cdot}$], singlet oxygen [$^1O_2$], and hydrogen peroxide [H_2O_2]) as well as reactive nitrogen species (e.g., nitrosonium cation [NO^+], nitroxyl anion [NO^-], and peroxynitrite [$ONOO^-$] [16–18]). These free radical and nonradical species react with several amino acid residues altering their structures and, by extension, the tertiary structures of the parent protein. In the case of RyR2, changes in its tertiary structure will alter its sensitivity to endogenous ligands like calcium and ATP. It is also possible that by altering the oxidative environment, radical species could promote oxidation of sulfhydryl groups leading to formation of additional disulfide bonds on RyR2. In a recent study, we found that in vitro treatment of RyR2 from 6-week diabetic rat hearts with 2 mmol/l dithiothreitol partially restored its ability to bind [^{3}H]ryanodine (19). These data are consistent with the notion that the dysfunction of RyR2 stems from diabetes-induced increases in disulfide bond formation. However, at this

time, it is uncertain which of the 90 cysteine residues on each RyR2 monomer are modified and how many of these disulfide bonds are formed intra-monomer and how many are formed inter-monomer.

Second, it is known that elevation in circulating levels of aldose and ketose sugars brought on by diabetes accelerates the formation of Schiff bases on lysine, arginine, or histidine residues (nonenzymatic glycation reactions [16,20]). Over time (~24–48 h), Schiff bases undergo internal rearrangement to form more stable Amadori products (21). On long-lived proteins such as ryanodine receptors (22), Amadori products rearrange further to form advanced glycation end products (AGEs) (23,24). Once formed, these complex molecules remain attached to the protein throughout its lifetime. Studies have shown that modification of proteins with nonenzymatic glycation products precipitates tissue and ultimately organ dysfunction (25,26).

The present study was initiated to determine whether non–cross-linking AGEs are formed on RyR2 during chronic diabetes and if formation of these post-translational modifications could be minimized or attenuated with 2 weeks of insulin treatment, initiated after 6 weeks of diabetes.

RESEACH DESIGN AND METHODS

Chemicals and drugs. STZ, iodoacetamide, trifluoroacetic acid, α-cyano-4-hydroxycinnamic acid, and dithiothreitol were obtained from Sigma-Aldrich (St. Louis, MO). Trypsin was obtained from Promega (Madison, WI). Mouse monoclonal anti-RyR2 antibodies were obtained from Affinity Bioreagents (Golden, CO). Actin antibodies (C-11) were purchased from Santa Cruz Biotechnology (Santa Cruz, CA). Restriction enzymes (*Bso*BI, *Eco*NI, and *Nhe*I) were obtained from New England Biolabs (Beverly, MA). Ryanodine was isolated from chipped *Ryania* wood supplied by Integrated Biotechnology (Carmel, IN) and purified by chromatography to ≥98%. [^{3}H]ryanodine (specific activity 56 Ci/mmol) was purchased from Perkin Elmer-Life Science Products (Boston, MA). Brevital (methohexital sodium) and NPH Ilentin II (intermediate-acting insulin) were obtained from Eli Lilly (Indianapolis, IN). Oligo primers were obtained from Integrated DNA Technologies (Coralville, IA). Other reagents and solvents used were of analytical grade.

Induction and verification of experimental STZ-induced diabetes. All animal procedures were carried out in accordance with guidelines established by institutional animal care and use committees. Male Sprague-Dawley rats (Harlan Laboratories, Indianapolis, IN) weighing between 180 and 190 g were anesthetized with Brevital (25 mg/kg i.p.) and then injected via a tail vein with a single dose of either STZ in 0.1 mol/l citrate buffer, pH 4.5 (50 mg/kg), or citrate buffer. Three days later, blood glucose levels were determined using a Glucometer II and Glucostix (Peridochrom Glucose GOD-PAP Assay Kit; Roche Molecular Biochemicals, Indianapolis, IN) to establish induction of diabetes. Animals with blood glucose levels <15 mmol/l were injected with a second dose of STZ. Throughout this study, animals were housed in pairs (similar weights to minimize dominance) at 22°C with fixed 12-h light/12-h dark cycles and given free access to food and water. Blood glucose and body weights were monitored weekly.

Insulin treatment protocols. Six weeks after the STZ injection, diabetic animals were randomly divided into two subgroups. One of the subgroups was placed on an insulin regimen for 2 weeks. For these animals, insulin doses were individually adjusted to maintain the euglycemic state and varied between 12 and 16 units/kg s.c., given once per day between 9:00 and 11:00 A.M. The other subgroup of diabetic animals continued as nontreated diabetics for 2 additional weeks. Diabetic animals whose body weight fell below 90% of initial starting body weight during the in vivo protocol were killed and eliminated from the study. This experimental protocol afforded 8-week age-matched control (8C), 8-week STZ-induced diabetic (8D), and 6-week STZ-induced diabetic/2-week insulin-treated (6D-2I) animals.

Sample collection. At the end of the in vivo procedure, animals were anesthetized with a single lethal dose of Brevital (75 mg/kg i.p.). Abdominal cavities were opened, and blood samples were collected via left renal arteries (27) for analysis of whole blood glucose, insulin, and HbA_{1c} content. Chest cavities were then opened and hearts were removed and quick-frozen by embedding in crushed dry ice. Frozen hearts from each of 8C, 8D, and 6D-2I were then divided into two subgroups of three and six hearts each. Hearts in the smaller subgroup were used to determine levels of mRNA encoding RyR2, whereas the larger subgroup of six hearts was used for determination of RyR2 protein and function.

Quantitation of mRNA encoding RyR2 in 8C, 8D, and 6D-2I rat hearts. A detailed procedure for determining RyR2 mRNA content is described elsewhere (14,15). Briefly, total RNA was extracted separately but simultaneously from 8C, 8D, and 6D-2I rat hearts using Quick Prep total RNA extraction kits (Amersham Pharmacia Biotech, Piscataway, NJ). At the end of the procedure, extracted RNA was suspended in 1 ml of slightly alkaline diethylpyrocarbonate-treated water (pH 7.5), and concentrations were determined spectrophotometrically at 260 nm. Thereafter, equivalent amounts of RNA from each of 8C, 8D, and 6D-2I were used to synthesize first-strand cDNA. PCRs were then carried out to amplify cDNAs encoding RyR2 using β-actin as an internal reference. Primers for RyR2 were as follows: sense (5′-GTGTTTGGATCCTCTGCAGTTCAT-3′) and anti-sense (5′-AGAGGCA CAAAGAGGAATTCGG-3′); whereas those for β-actin were as follows: sense (5′-CGTAAAGACCTCTATGCCA-3′) and anti-sense (5′-AGCCATGCCAAAT GTCTCAT-3′).

Quantitation of the mRNA encoding receptor for AGEs in 8C, 8D, and 6D-2I rat hearts. RT-PCR was carried out to determine the levels of mRNA encoding the receptor for AGEs (RAGE) as well as a major spliced variant of RAGE in 8C, 8D, and 6D-2I. A single pair of primers was used to determine RAGE as well as its splice variant. This primer pair was selected from sequences (GenBank accession number L33413 for RAGE) 5′ and 3′ of the intron that generates the variant and are as follows: sense (5′-AGGTGGAA CAGTCGCTCC-3′) and anti-sense (5′-CACAGCTGAGGTCGGAAC-3′).

Determination of amount of RyR2 protein in 8C, 8D, and 6D-2I rat hearts. As described previously, two sequential steps were used to determine the relative levels of RyR2 protein in 8C, 8D, and 6D-2I rat hearts (14,15). First, membrane vesicles were prepared simultaneously from control, STZ-induced diabetic, and insulin-treated rat hearts (three hearts per preparation × two preparations), and their protein content was determined using the method of Lowry et al. (28). Second, 100 μg total protein from each vesicle preparation was solubilized in gel dissociation medium containing 10 mg/ml dithiothreitol and electrophoresed for 3.5 h at 150 V using denaturing 4–20% linear gradient polyacrylamide gels. Various amount of purified RyR2 protein (50–350 ng) were simultaneous run in parallel lanes on the same gel to serve as a calibration curve. Gels were then stained with Coomassie blue dye, destained overnight, and dried between two sheets of cellophane. The intensity of the RyR2 band in each vesicle preparation was then determined by interpolation on the calibration curve derived from various RyR2 concentrations. Western blot analyses were also carried out as described previously (14,15) to confirm relative levels of RyR2 protein in each vesicle preparation. For these experiments, β-actin served as an internal control to correct for sample loading.

Ability of RyR2 from 8C, 8D, and 6D-2I rat hearts to bind [^{3}H]ryanodine. The functional integrity of RyR2 from each of 8C, 8D, and 6D-2I was assessed from its ability to bind [^{3}H]ryanodine (14,15). For this, 100 μg/ml of membrane vesicle protein from 8C, 8D, and 6D-2I were incubated in binding buffer containing 200 μmol/l free calcium (500 mmol/l KCl, 20 mmol/l Tris-HCl, 300 μmol/l $CaCl_2$, 0.1 mmol/l EGTA, 6.7 nmol/l [^{3}H]ryanodine, pH 7.4) for 2 h at 37°C. After incubation, vesicles were filtered and washed, and the amount of [^{3}H]ryanodine bound to RyR2 was determined by liquid scintillation counting. Nonspecific binding was determined simultaneously by incubating vesicles with 1 μmol/l unlabeled ryanodine.

The affinities of ryanodine for RyR2 from 8C, 8D, and 6D-2I were determined using binding assays. These experiments were conducted as described above except that increasing concentrations of unlabeled ryanodine (0–300 nmol/l) were also added to the samples. Equilibrium dissociation constant (K_d) values were ascertained using the Cheng-Prusoff relationship (29) given by the following:

$$K_d = IC_{50}/[1 + (L)/K_L] \quad (1)$$

where IC_{50} is the concentration that displaces 50% of [^{3}H]ryanodine, L is the concentration of [^{3}H]ryanodine used (6.7 nmol/l), and K_L is the K_d of [^{3}H]ryanodine (1.2 nmol/l for RyR2 [30]).

Binding affinity experiments were also carried out to determine whether the calcium sensitivity of RyR2 is altered by diabetes. For this, 100 μg/ml vesicle protein from 8C, 8D, and 6D-2I were incubated in binding buffer (500 mmol/l KCl, 20 mmol/l Tris-HCl, 0.1 mmol/l EGTA, and 6.7 nmol/l [^{3}H]ryanodine, pH 7.4) containing various amounts of free calcium (1–3,000 μmol/l) for 2 h at 37°C. After incubation, vesicles were filtered and washed, and the amount of [^{3}H]ryanodine bound to RyR2 was determined using liquid scintillation counting. Nonspecific binding was determined simultaneously by incubating vesicles with 1 μmol/l unlabeled ryanodine.

Determination of glycation products on RyR2 from 8C, 8D, and 6D-2I rat hearts. Membrane vesicles prepared from control, diabetic, and insulin-treated rat hearts were electrophoresed using denaturing SDS-PAGE for 3.5 h (one gel for each membrane preparation from 8C, 8D, and 6D-2I). At the end of this time, the gels were stained with Coomassie blue dye and destained, and the bands corresponding to RyR2 were excised and transferred to 1.5 ml Eppendorff tubes containing distilled deionized water. Two sequential steps were then conducted to determine the presence of glycation products on RyR2.

In-gel protein digestion. Coomassie-stained RyR2 protein bands from 8C, 8D, and 6D-2I gels were cut into small pieces, destained with 50% acetonitrile/50 mmol/l ammonium bicarbonate, reduced with 10 mmol/l dithiothreitol, and then alkylated with 55 mmol/l iodoacetamide. After alkylation, the gel pieces were digested overnight with trypsin (6 ng/nl; Promega) at 37°C. The next day, the peptides were desalted by eluting from micro C_{18} ZipTip columns (Millipore, Bedford, MA) with a solution of 50% acetonitrile and 0.1% trifluoroacetic acid. α-Cyano-4-hydroxycinnamic acid was used as the matrix.

Mass spectrometry analysis. First, matrix-assisted laser desorption ionization–time of flight (MALDI-TOF) mass spectrograms were recorded in the positive reflectron mode (Micromass, Manchester, U.K.). Time of flight was measured using the following parameters: 3,400 V pulse voltage, 15,000 V source voltage, 500 V reflectron voltage, 1,950 V multichannel plate (MCP) voltage, and low mass gate of 500 Da. Internal calibration was performed using auto digestion peaks of bovine trypsin (monoisotopic mass $[M+H^+]$, m/z 842.5099 and m/z 2211.1045) before analysis of experimental samples. Second, liquid chromatography–mass spectrometry analyses of digested RyR2 peptides from 8C and 8D were also performed using a capillary liquid chromatography system coupled with a quadruple time of flight (Q-TOF) mass spectrometer (Micromass) fitted with a Z-spray ion source. Samples were desalted and concentrated using an online pre-column (C_{18}, 0.3 mm i.d., 5 mm length). Separation of the peptides was carried out on a reverse-phase capillary column (Pepmap C_{18}, 75 mm i.d., 15 cm length; LC Packings, San Francisco, CA) running at 300 nl/min. The mobile phase consisted of a linear gradient from 100% solution A (0.1% formic acid/3% acetonitrile/96.9% H_2O, vol/vol) to 70% solution B (0.1% formic acid/2.9% H_2O/97% acetonitrile, vol/vol) for 50 min followed by a 10-min gradient to 100% solution B. Mass spectra were acquired in positive ion mode.

Identification of glycation products on RyR2 from 8C, 8D, and 6D-2I rat hearts. Mass data files obtained from MALDI-TOF analyses of RyR2 from 8C, 8D, and 6D-2I were then search using an in-house PERLscript algorithm for $M+H^+$ peaks corresponding to theoretical RyR2 peptides with one lysine or arginine miscleavage (or no miscleaved peptide with a histidine residue within) that have been modified with a single N^{ε}-(carboxymethyl)-lysine, imidazolone A, imidazone B, pyrraline, or 1-alkyl-2-formyl-3,4-glycosyl pyrrole molecule (AFGP) functionality.

Data analyses. Differences between values from each of 8C, 8D, and 6D-2I rat hearts were evaluated by one-way ANOVA followed by the Newman-Keuls test. The data shown are means ± SE. Results were considered significantly different at $P < 0.05$.

RESULTS

Induction of experimental STZ-induced diabetes. Mean body weight of all animals at the start of the study was 184.2 ± 2.0 g. During the in vivo procedure, mean body weights of control animals increased progressively, reaching 413 ± 4.0 g on 56 days. Mean body weight of animals injected with 50 mg/kg STZ increased minimally over this period (to 201 ± 2.7 g on day 56). It should be pointed out that, whereas diabetic animals did not gain as much weight as control animals, there was no body wasting. These animals showed typical signs of type 1 diabetes, including polyuria, polyphagia, and polydipsia, but fed normally and moved around in their cages freely. Two weeks of insulin treatment initiated after 6 weeks of diabetes partially prevented or minimized weight loss induced by diabetes (mean body weight of insulin-treated animals was 281.5 ± 15.2 g on day 56).

At the beginning of the study, the average whole blood glucose level of all animals was 4.2 ± 0.2 mmol/l. For those animals injected with citrate buffer only (controls), mean blood glucose levels remained essentially unchanged throughout the 56-day study. However, blood glucose levels of animals injected with 50 mg/kg STZ increased to 20.1 ± 0.4 mmol/l after 3 days and increased progressively thereafter to ~29.4 mmol/l. Daily insulin treatment initiated after 6 weeks of diabetes normalized blood glucose levels to near control values. Heart weight to body weight ratios were also significantly higher in 8D when compared with 8C (4.5 vs. 2.7 mg/g). This ratio returned to near control values with insulin treatment (3.6 mg/g). Other characteristics of the animals used in this study are listed in Table 1.

TABLE 1
Some other characteristics of the animals at the end of the in vivo study

Parameter	8C	8D	6D-2I
n	12	12	12
Heart weight (g)	1.1 ± 0.1	0.9 ± 0.2	1.0 ± 0.1
Blood glucose (mmol/l)	3.9 ± 0.3	29.2 ± 1.4*	9.1 ± 2.7
Insulin (ng/ml)	2.4 ± 0.4	0.5 ± 0.2*	5.9 ± 2.0
HbA_{1c} (%)	4.1 ± 0.1	9.4 ± 0.7*	5.6 ± 0.5

Data are means ± SE. *Significantly different from control and insulin-treated animals.

Quantitation of mRNA encoding RyR2 from 8C, 8D, and 6D-2I rat hearts. Before proceeding with biochemical studies, modified Langendorff procedures were used to functionally establish the presence of diabetic cardiomyopathy in these animals. These data are shown elsewhere (15). mRNA encoding RyR2 was quantitated using RT-PCR employing β-actin as an internal reference. As shown in Fig. 1, after normalizing to concomitant β-actin, transcription of mRNA encoding RyR2 decreased by 24.2 ± 1.3% ($P < 0.05$) after 8 weeks of STZ-induced diabetes when compared with age-matched controls. Two weeks of insulin treatment, initiated after 6 weeks of STZ-induced diabetes, minimized and/or prevented loss in

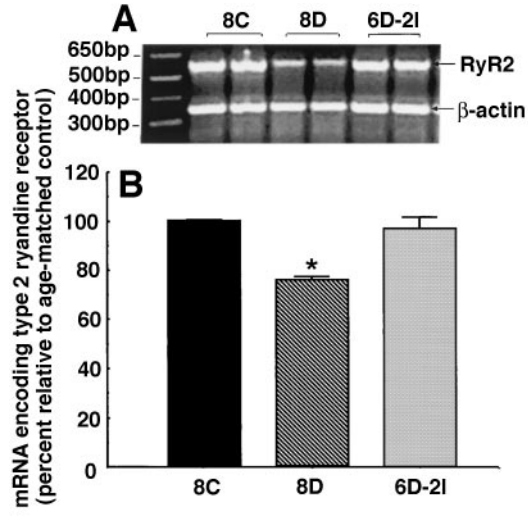

FIG. 1. Relative levels of RyR2 mRNA in hearts from 8C, 8D, and 6D-2I. Briefly, total RNA was reverse-transcribed into first-strand cDNA using oligo dT_{15} and Superscript II. Thereafter, specific primers were used in PCRs to amplify segments of cDNA encoding RyR2 and β-actin. *A* shows a typical electrophoretogram of RyR2 from 8C, 8D, and 6D-2I. The sizes of the products are as expected: 602 bp for RyR2 and 387 bp for β-actin. *B* shows the average data (means ± SE) for four experiments done in duplicate using three different cDNA preparations. *Significantly different from 8C and 6D-2I.

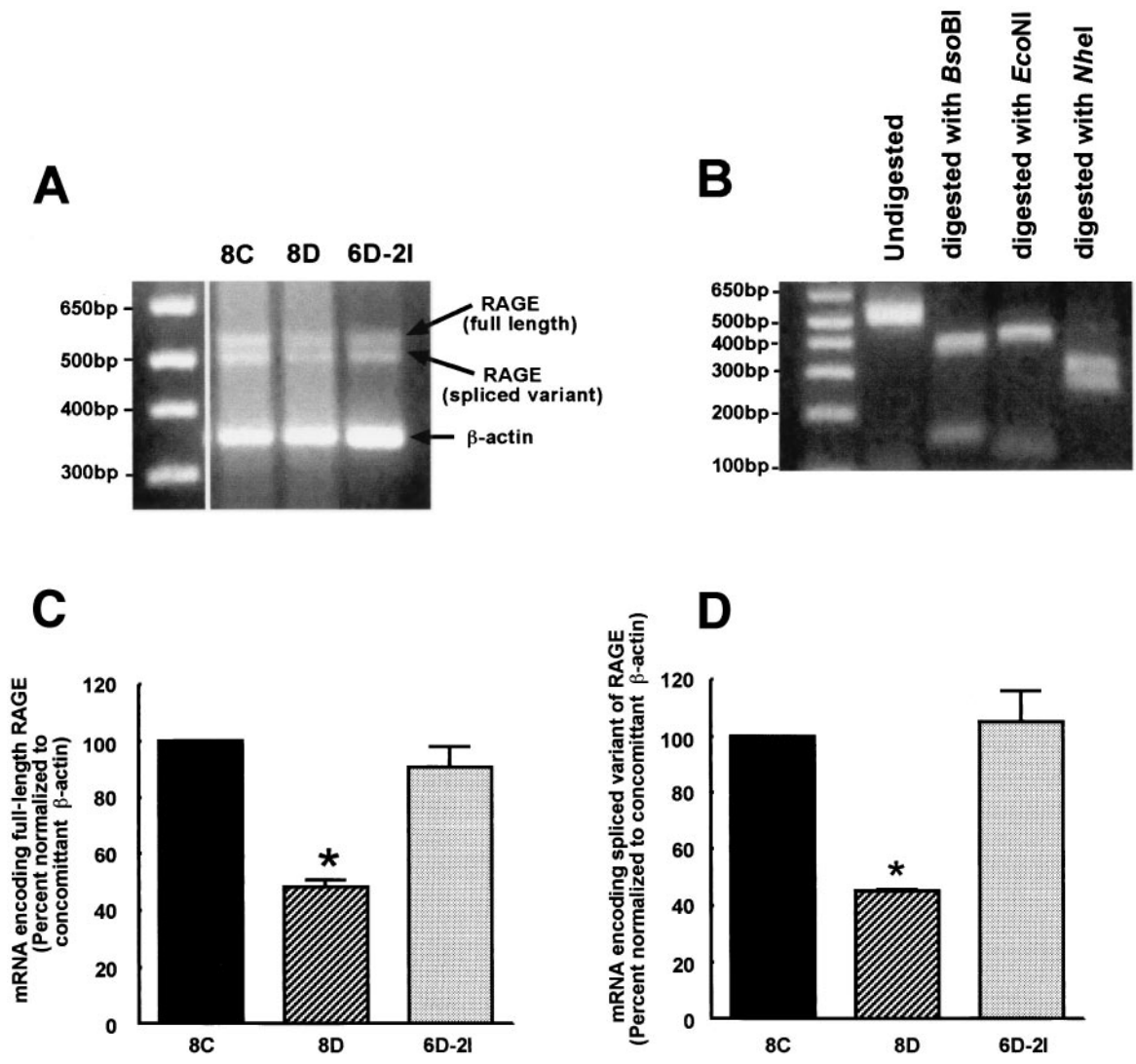

FIG. 2. Relative levels of RAGE mRNA in hearts from 8C, 8D, and 6D-2I. Briefly, total RNA was reverse-transcribed into first-strand cDNA using oligo dT_{15} and Superscript II. Thereafter, specific primers were used in PCRs to amplify segments of cDNA encoding RAGE and β-actin. *A* shows a typical electrophoretogram for RAGE from 8C, 8D, and 6D-2I. Products are of the expected sizes: 529 bp for full-length RAGE, 502 bp for the major splice variant of RAGE, and 387 bp for β-actin. *B* shows the restriction mapping data used to confirm the identity of RAGE. Digestion with *Bso*BI, *Eco*NI, and *Nhe*I afforded the predicted product sizes of 374 and 155, 420 and 127, and 286 and 243 bp. *C* and *D* show the average data (means ± SE) for four experiments done in duplicate using three different cDNA preparations to quantitate mRNA encoding RAGE (*C*) and its splice variant (*D*). *Significantly different from 8C and 6D-2I.

transcription of RyR2 mRNA (96.9 ± 4.4% of control, $P > 0.05$). These data are consistent with previous studies showing that transcription of mRNA encoding RyR2 decreases with diabetes, and this decrease was prevented or minimized with insulin treatment (11,14,15).

Quantitation of mRNA encoding RAGE from 8C, 8D, and 6D-2I rat hearts. mRNA encoding the full-length and a major spliced variant of rat RAGE (31) was determined using RT-PCR using a single pair of gene-specific oligo primers along with β-actin as an internal reference. In this study, we found that after normalizing to concomitant β-actin, transcription of mRNA encoding full-length RAGE decreased by 51.6 ± 2.3% ($P < 0.05$) after 8 weeks of diabetes when compared with age-matched controls (Fig. 2*A* and *C*). Similarly, transcription of mRNA encoding a major spliced variant of RAGE also decreased after 8 weeks of diabetes (54.8 ± 0.6%, $P < 0.05$, Fig. 2*A* and *D*). Restriction mapping confirmed the identity of these PCR products (Fig. 2*B*). Two weeks of insulin treatment, initiated after 6 weeks of STZ-induced diabetes, prevented or minimized loss in transcription of mRNA encoding full-length as well as the major spliced variant of RAGE (90.6 ± 7.3 and 104.9 ± 11.3% of age-matched controls, respectively).

Determination of the amount of RyR2 protein in 8C, 8D, and 6D-2I rat hearts. Membrane vesicles (100 μg) from 8C, 8D, and 6D-2I were solubilized in gel dissociation medium and electrophoresed on 4–20% linear gradient SDS-polyacrylamide gels as described above and elsewhere (14,15). The intensity of the RyR2 protein band in each sample was then interpolated on RyR2 calibration curves (run simultaneously on the same gels) to determine RyR2 content. Using this method, membrane vesicles from 8D contained 34.7% less RyR2 protein than those from 8C [124.8 ± 17.0 ng RyR2 protein/100 μg of membrane vesicles compared with 194.2 ± 22.1 ng RyR2 protein/100 μg of

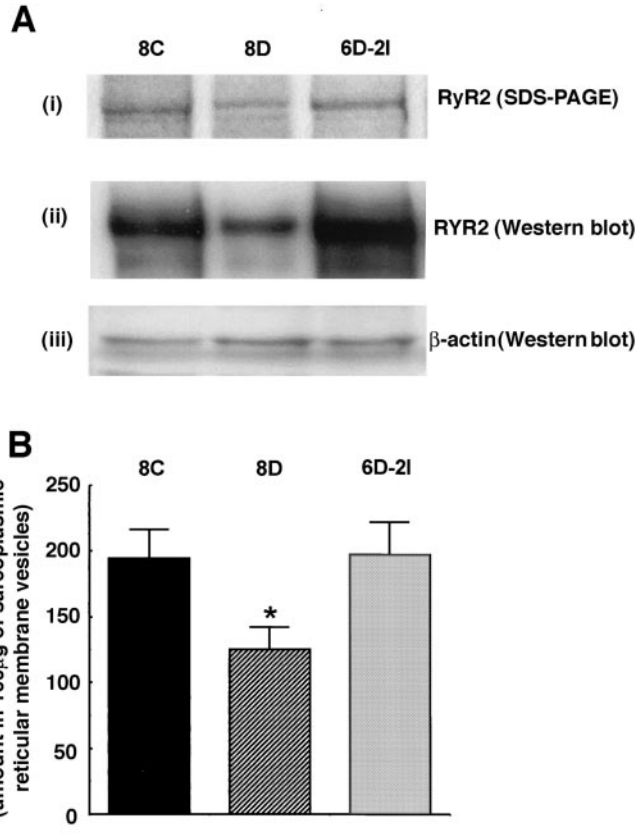

FIG. 3. Relative levels of RyR2 protein in 100 μg of membrane vesicles from 8C, 8D, and 6D-2I rat hearts. *A*(i) shows a typical SDS-PAGE electrophoretogram for RyR2 from 8C, 8D, and 6D-2I. Note the slowing in the electrophoretic mobility of RyR2 from 8D. *A*(ii) shows a typical autoradiogram from Western blot analysis of RyR2 from 8C, 8D, and 6D-2I, confirming relative protein levels. *A*(iii) shows a typical autoradiogram from Western blot analysis for β-actin from 8C, 8D, and 6D-2I. This protein was used as a control to correct for sample load. *B* shows the average data (means ± SE) from four experiments done in duplicate using two different membrane preparations to quantitate relative levels of RyR2 protein. *Significantly different from 8C and 6D-2I.

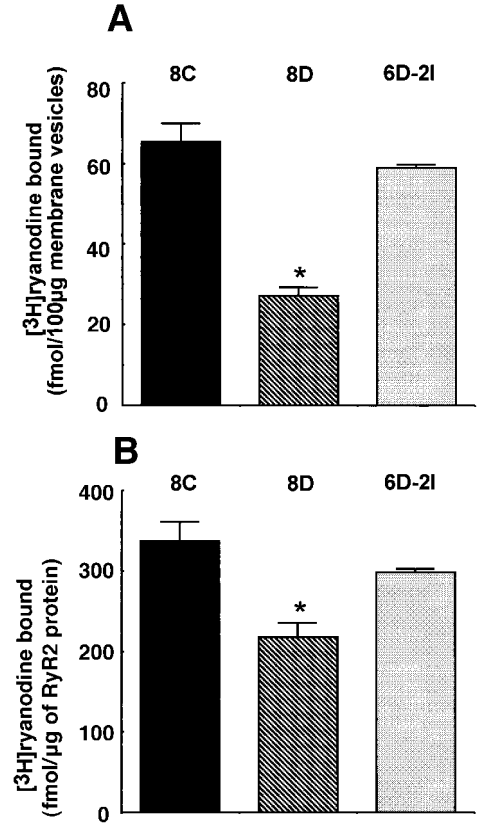

FIG. 4. [^{3}H]ryanodine binding to membrane vesicles from 8C, 8D, and 6D-2I rat hearts. *A*: Membrane vesicles (0.1 mg/ml) from 8C, 8D, and 6D-2I were incubated for 2 h at 37°C with 6.7 nmol/l [^{3}H]ryanodine in binding buffer consisting of 500 mmol/l KCl, 0.3 mmol/l $CaCl_2$, 0.1 mmol/l EGTA, and 20 mmol/l Tris-HCl (pH 7.4). After incubation, the vesicles were filtered and washed, and [^{3}H]ryanodine bound to RyR2 was determined by liquid scintillation counting. Data shown are means ± SE for at least six experiments done using two different membrane preparations. *Significant difference between control and insulin-treated preparations. *B*: [^{3}H]ryanodine bound to 1 μg RyR2 from 8C, 8D, and 6D-2I rat hearts. The amount of RyR2 in 100 μg of membrane vesicles was determined by interpolation on RyR2 calibration curves. The amount of [^{3}H]ryanodine bound was then normalized per microgram of RyR2 protein. Values shown are means ± SE for at least six experiments done using two different membrane preparations. *Significantly different from 8C and 6D-2I.

membrane vesicles, respectively; see Fig. 3*A*(i) and *B*]. This amount was significantly different. These data were then confirmed using Western blot analyses employing β-actin as an internal control [Fig. 3*A*(ii) and (iii)] and are consistent with previous studies showing that expression of RyR2 decreases with diabetes (15). Using this method, we also found that membrane vesicles from 6D-2I rat hearts contained 197.5 ± 24.3 ng RyR2 protein/100 μg of membrane vesicles (see Fig. 3*B*, third bar graph on the right). Consistent with previous findings, these data suggest that 2 weeks of insulin treatment is able to minimize and/or prevent loss of expression of RyR2 induced by diabetes.

Ability of RyR2 from 8C, 8D, and 6D-2I rat hearts to bind [^{3}H]ryanodine. The functional integrity of RyR2 from 8C, 8D, and 6D-2I was assessed from its ability to bind the specific ligand [^{3}H]ryanodine. As shown in Fig. 4*A*, 100 μg of membrane vesicles from 8D bound 58.4% less [^{3}H]ryanodine when compared with age-matched controls (27.2 ± 2.2 vs. 65.4 ± 4.6 fmol [^{3}H]ryanodine/100 μg of membrane vesicles), whereas vesicles from 6D-2I bound 11.0% less [^{3}H]ryanodine than age-matched controls (58.8 ± 1.0 fmol [^{3}H]ryanodine/100 μg of membrane vesicles). Because the amount of RyR2 in each membrane preparation differed, the amount of [^{3}H]ryanodine bound was normalized to a fixed amount of RyR2 protein. As shown in Fig. 4*B*, after normalization per microgram of protein, RyR2 from 8D still bound 34.4% less [^{3}H]ryanodine than RyR2 from age-matched controls (217.5 ± 17.6 vs. 336.6 ± 24.1 fmol [^{3}H]ryanodine/μg RyR2, $P < 0.05$). These data are consistent with our previous findings showing that at a fixed amount, RyR2 protein from diabetic rat hearts bind less [^{3}H]ryanodine (i.e., RyR2 become dysfunctional [14,15]). On the other hand, RyR2 from insulin-treated animals bound 10.4% less [^{3}H]ryanodine than controls (297.8 ± 4.7 fmol [^{3}H]ryanodine/μg RyR2, $P > 0.05$). In these experiments, 2 weeks of insulin treatment partially restored RyR2's ability to bind [^{3}H]ryanodine.

Affinity of RyR2 from 8C, 8D, and 6–2I rat hearts for ryanodine. Equilibrium displacement binding affinity assays were used to determine the affinity of RyR2 for ryanodine. In these assays, unlabeled ryanodine displaced [^{3}H]ryanodine from control RyR2 in a concentration-dependent manner, exhibiting an IC_{50} of 4.4 ± 0.4 nmol/l.

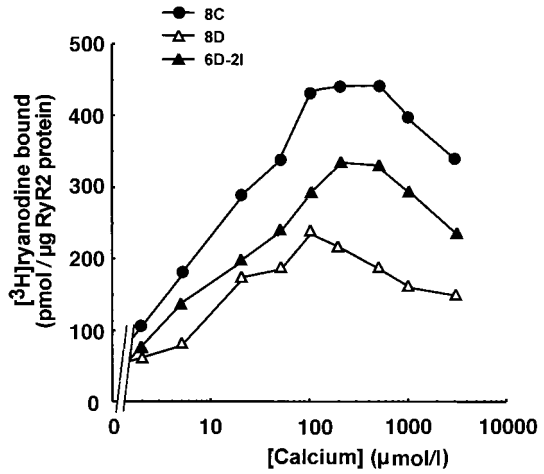

FIG. 5. Effect of calcium on the ability of RyR2 from 8C, 8D, and 6D-2I rat hearts to bind [^{3}H]ryanodine. Binding affinity assays were used to determine the effect of diabetes on the sensitivity of RyR2 to calcium. Briefly, 100 μg of membrane vesicles from 8C, 8D, and 6D-2I were incubated for 2 h at 37°C in the presence of 6.7 nmol/l [^{3}H]ryanodine and various concentrations of free calcium (1–3,000 μmol/l) in a buffer consisting of 500 mmol/l KCl, 20 mmol/l Tris-HCl, and 0.1 mmol/l EGTA (pH 7.4 at 37°C). At the end of the incubation, the vesicles were filtered and washed. [^{3}H]ryanodine bound to the receptors was determined by liquid scintillation counting. Data shown represent the mean for at least four experiments done using two different membrane preparations. Standard errors were <10% and were not included for clarity of data.

Unlabelled ryanodine also displaced [^{3}H]ryanodine from diabetic and insulin-treated RyR2 in concentration-dependent manners (IC_{50} of 3.3 ± 0.2 nmol/l and IC_{50} of 4.3 ± 0.4 nmol/l, respectively). These IC_{50} values were not significantly different from controls. The slight leftward shift of the displacement curve for RyR2 from 8D is consistent with the membrane preparation having a lower RyR2 protein content. Using the algorithms of GraphPad Prism 3.0a (GraphPad Software, San Diego CA), displacement binding data for 8C, 8D, and 6D-2I fitted best to a single binding site model (r^2 = 0.86–0.96). Using the Cheng-Prusoff equation (Eq. 1 in RESEARCH DESIGN AND METHODS), the K_d values for ryanodine were 0.7 ± 0.1 nmol/l for 8C, 0.5 ± 0.1 nmol/l for 8D, and 0.7 ± 0.1 nmol/l for 6D-2I.

Calcium sensitivity of [^{3}H]ryanodine binding by RyR2 from 8C, 8D, and 6D-2I rat hearts. Experiments were also conducted to determine whether the sensitivity of RyR2 to calcium alters with diabetes. The response of RyR2 to calcium concentration was evaluated from its ability to bind [^{3}H]ryanodine, because the amount of [^{3}H]ryanodine bound is a direct measure of the "openness" of these channels (32). In this study, [^{3}H]ryanodine bound was normalized per microgram RyR2 protein for each of the different preparations. As shown in Fig. 5 (●), the amount of [^{3}H]ryanodine bound to control RyR2 was biphasic as the concentration of calcium varied from 1 to 3,000 μmol/l. Between concentrations of 1 and 100 μmol/l calcium, [^{3}H]ryanodine binding increased linearly and then plateaued between 200 and 500 μmol/l, reaching a maximum of 441.4 ± 16.3 pmol [^{3}H]ryanodine bound/μg RyR2 protein. As the concentration of buffered free calcium increased beyond 500 μmol/l, the amount of [^{3}H]ryanodine bound to RyR2 from 8C decreased, suggesting that the channel becomes deactivated. RyR2 from 8D also exhibited the typical biphasic response to calcium, but with three notable differences. First, the maximum amount of [^{3}H]ryanodine bound to RyR2 from 8D was 46.9% less than that bound by 8C (234.4 ± 10.5 pmol [^{3}H]ryanodine bound/μg RyR2 compared with 441.4 ± 16.3 pmol [^{3}H]ryanodine bound/μg RyR2). Second, peak [^{3}H]ryanodine binding occurred at 100 μmol/l calcium for RyR2 from 8D compared with 500 μmol/l for RyR2 from 8C. Third, concentrations of calcium >100 μmol/l rapidly deactivated or closed RyR2 from 8D, as indicated from its decreased ability to bind [^{3}H]ryanodine. These data show for the first time that diabetes alters the sensitivity of RyR2 to calcium.

The calcium response of RyR2 from 6D-2I mirrored that of 8C with one exception: the maximum [^{3}H]ryanodine bound (B_{max}) was lowered to 335.5 ± 12 pmol [^{3}H]ryanodine/μg RyR2 protein (24% decreased; Fig. 5 [▲]). Thus, 2 weeks of insulin treatment restored calcium sensitivity to RyR2 but only partially restored its ability to bind [^{3}H]ryanodine.

Trypsin digestion of RyR2 from 8C, 8D, and 6D-2I rat hearts and determination of peptide masses. Membrane vesicles prepared from hearts of 8C, 8D, and 6D-2I were electrophoresed using denaturing SDS-PAGE. At the end of the separation, the gels were stained with Coomassie blue dye and destained, and the bands corresponding to RyR2 were excised, washed, and digested overnight with trypsin. The $M+H^+$ values of the peptides were then determined using MALDI-TOF and nanoflow-ESI-Q-TOF. It should be mentioned that although the complete cDNA encoding rat RyR2 is not available, this protein is highly conserved among species, and its amino acid sequence is expected to be similar to those published for mouse, rabbit, and human RyR2, which all share >92% homology. In addition, to avoid ambiguity in our analyses, only consensus RyR2 sequences from mice, rabbits, and humans were investigated, because these said sequences are likely to be present on rat RyR2.

Digestion of RyR2 from 8C with trypsin afforded 298 peptides with $M+H^+$ values between 500 and 3000 Da. Peptides with $M+H^+$ >3000 Da were not detected probably because of their low ionization efficiencies and large size (unable to escape from the gel). Of these 298 peptides, at least 136 corresponded to non-miscleaved consensus trypsin peptides from mouse, rabbit, and human RyR2 proteins (140 or 46.7% from mouse RyR2, 144 or 48.3% from rabbit RyR2, and 136 or 45.6% from human RyR2). As shown in the middle panel of Fig. 6*A*, these peptides spanned the entire range of rabbit RyR2, with minimum variability (≤595 parts per million, right panel). Digestion of RyR2 from 8D with trypsin afforded 20.8% fewer peptides compared with 8C. This reduction in peptides suggests that changes are occurring to RyR2 in such a manner as to compromise trypsin's ability to digest it. Because trypsin cleaves at lysine and arginine residues, it is logical to conclude that modifications are occurring at these residues.

If adducts are being formed on lysine and/or arginine residues, then miscleavages are also likely to occur at these modified sites. As such, the peptide composition generated from digestion of RyR2 from 8D should not be completely represented as a subset of the peptides obtained from control RyR2. In fact, only 58 of the total

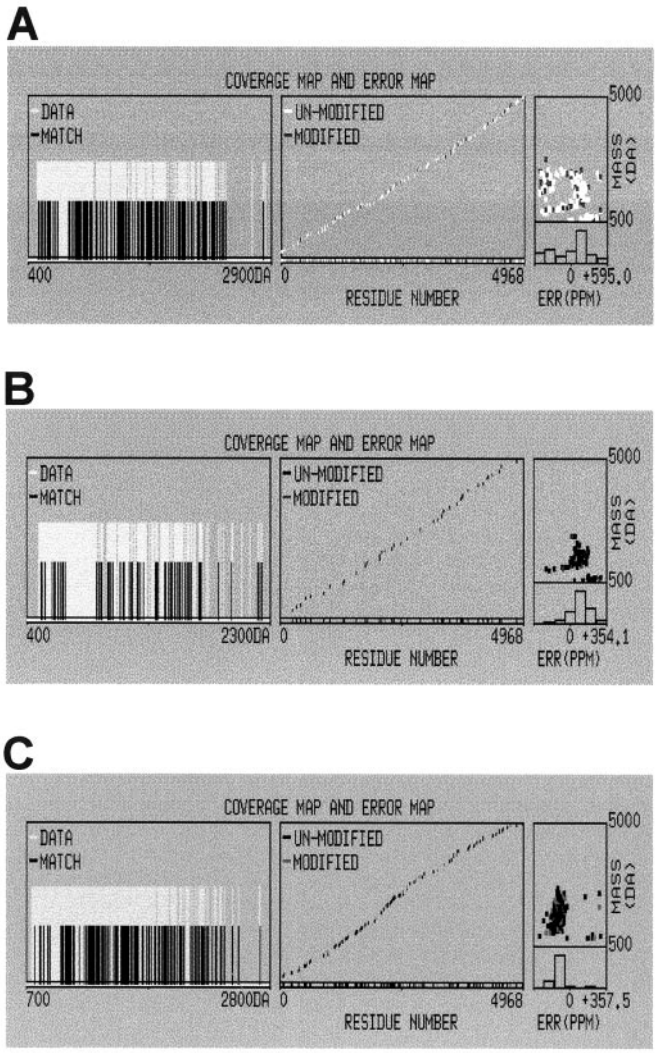

FIG. 6. Alignment of peptides obtained following digestion of RyR2 from 8C (*A*), 8D (*B*), and 6D-2I (*C*) rat hearts. Briefly, RyR2 from 8C, 8D, and 6D-2I was digested overnight with trypsin. The resultant peptides were then desalted and analyzed using MALDI-TOF mass spectrometry. The mass data files were then uploaded into the web-based program Profound (http://prowl.rockefeller.edu/cgi-bin/ProFound) to confirm the identity of the protein. The white vertical lines in the left panels of *A–C* reflect the total number of peptides obtained after trypsin digestion of RyR2 from 8C, 8D, and 6D-2I, respectively. The lower black lines in *A– C* represent peptides that are identical with peptides from rabbit RyR2. The middle panels in *A–C* show the distribution of the matched peptides throughout the entire span of rabbit RyR2 protein, whereas the right panels show the variability of the data. ERR, error; PPM, parts per million.

$M+H^+$ values obtained after digestion of RyR2 from 8D with trypsin corresponded to theoretical rabbit RyR2 peptides (63 corresponded to mouse RyR2 peptides and 64 to human RyR2 peptides). This reduction of matched peptides (60%) can be seen in the left (black lines) and middle panels of Fig. 6*B*. Likewise, the number of $M+H^+$ values that did not match known RyR2 peptides increased from 154 in 8C to 178 in 8D (an increase of 15.5%). When reverse-phase liquid chromatography was carried out using a capillary column coupled with a Q-TOF mass detector, diabetic RyR2 generated fewer peptides with retention times >40 min when compared with trypsin digestion of age-matched RyR2 (data not shown).

Digestion of RyR2 from 6D-2I with trypsin afforded 304 peptides with $M+H^+$ values ranging from 700 to 3000 Da. Of these, 124 corresponded to the masses of trypsin peptides from rabbit RyR2 (127 from mouse RyR2 and 118 from human RyR2). Interestingly, the $M+H^+$ values from 6D-2I that corresponded to peptides from RyR2 were also not wholly a subset of the $M+H^+$ values obtained from 8C (left panel of Fig. 6*C*). These data clearly suggest that 2 weeks of insulin treatment was able only to partially attenuate or minimize post-translational modifications on critical lysine and arginine residues on RyR2.

Identification of glycation products on RyR2. As mentioned above, the MALDI-TOF mass data files generated for RyR2 from 8D and 6D-2I were searched using an in-house PERLscript algorithm for $M+H^+$ values corresponding to theoretical RyR2 peptides with one miscleavage (or theoretical trypsin digested peptide containing a histidine residue within) modified with a single N^{ϵ}-(carboxymethyl)-lysine, imidazolone A, imidazone B, pyrraline, or AFGP. It should be pointed out that modifications found naturally in 8C were not included in the analysis since we were only interested in those modifications that resulted from diabetes. The structures of these non–cross-linking AGEs and their delta masses (Δ) are shown in Fig. 7.

As an example, search of MALDI-TOF mass files revealed monoisotopic masses of 1330.81 and 1330.47 Da that were prominent in 8D and 6D-2I samples but not in 8C (Fig. 8). MALDI-TOF analyses of 8D and 6D-2I were done on different days—hence the reason for the small shift in delta masses. Because no peptide generated from trypsin digestion of RyR2 (without or even with up to five miscleavages) possesses an $M+H^+$ of 1330.5 ± 0.5 Da, this $M+H^+$ reflects the mass of a peptide containing a modification. The next step was to determine the nature of the modification and which peptide fragment (amino acid) contained the adduct.

Three limiting parameters were used to search for data in this study: *1*) peptide fragments with only a single modification were allowed, *2*) peptides must contain either one missed cleavage at a lysine or arginine residue (or no miscleavage but containing a histidine residue), and *3*) only non–cross-linking modifications were included. Using these criteria, RyR2 from mice, rabbits, and humans were digested in silico (http://us.expasy.org/tools/peptidemass.html), and $M+H^+$ of all possible peptides (including cysteine modification with iodoacetamide and acrylamide adducts, oxidized methionines, and up to five miscleavages) were included. The data files from MALDI-TOF analyses were then searched using the PERLscript algorithm for peptides with $M+H^+$ values that were 58.02, 108.02, 142.03, 144.03, or 270.07 Da less than 1330.50 ± 0.5 Da. No $M+H^+$ values of 1272.47 (i.e., 1330.48 – 58.02), 1188.46, or 1186.46 Da were detected in the mass files, suggesting that these mass values do not correspond to masses of trypsin-derived peptides from RyR2. However, the mass files for RyR2 from 8C, 8D, and 6D-2I contained an $M+H^+$ of 1060.48 ± 0.1 Da. The latter corresponds to the mass of the miscleaved peptides, $_{1606}$VDVS**R**ISER$_{1614}$ and $_{4463}$L**R**QLTHTHR$_{4470}$. The subscript numbers represent the location of these peptides on RyR2 from mice, rabbits, and humans, and the bold letter indicates the amino acid involved in the modification. Therefore, the

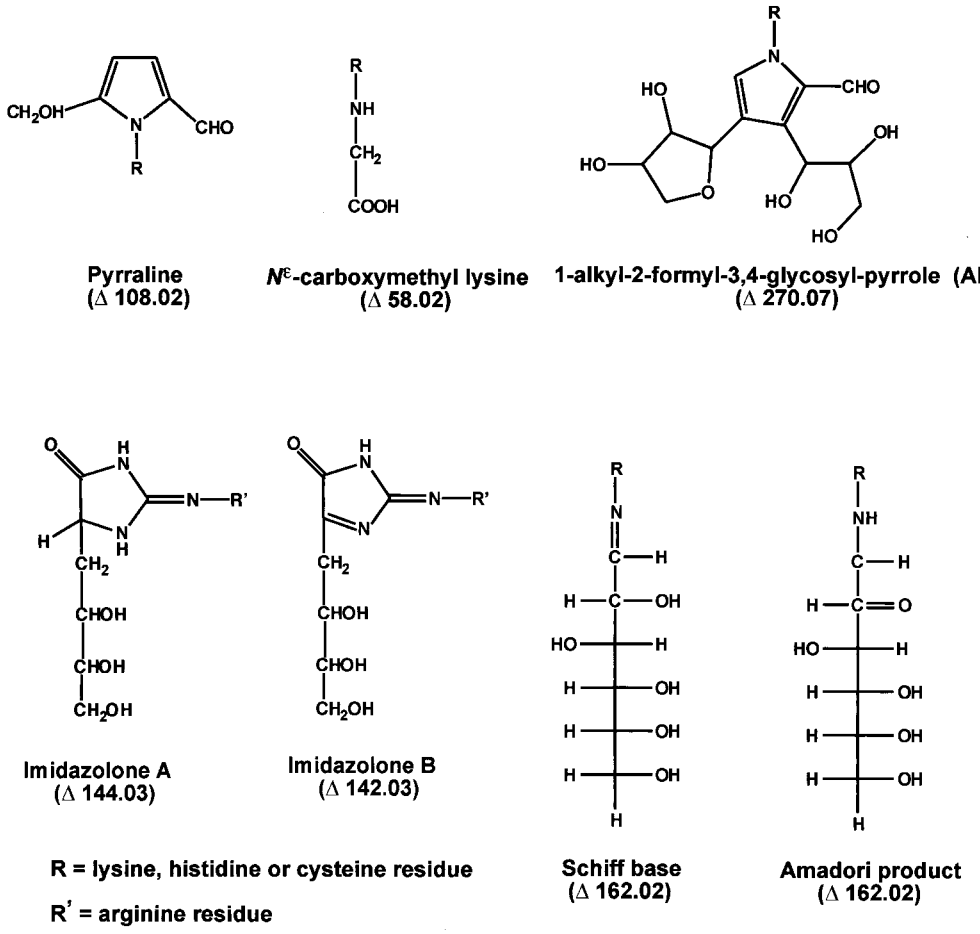

FIG. 7. Structures and the delta (Δ) masses of non–cross-linking AGE molecules and precursor Schiff bases and Amadori products assessed. Configurations were drawn using the algorithms of the software packages of CS Chem 3D Pro Version 5 (Cambridge Scientific Computing, Cambridge, MA).

$M+H^+$ values 1330.81 and 1330.47 seen in diabetic and insulin-treated RyR2 apparently resulted from a single AFGP modification on either arginine 1610 or arginine 4464. It is also likely that the $M+H^+$ of 1330.50 ± 0.5 Da could have resulted from a single pyraline modification (+108.02 Da) of $_{4677}$AALDFSDA**R**EK$_{4687}$ at arginine 4685. These data are the first to show not only that non–cross-linking AGEs are formed on RyR2 during diabetes, but also the type of modification as well as its precise location on RyR2.

Modifications were not always seen on peptides from both diabetic and insulin-treated RyR2. Several peptides from insulin-treated RyR2 contained modifications that were either less prominent or absent from RyR2 of 8D as well as RyR2 from 8C. As shown in Fig. 9, a $M+H^+$ of 1653.67 Da was prominent in insulin-treated diabetic RyR2, but not present in control and diabetic RyR2. Analysis of the theoretical mass files suggests that this $M+H^+$ could have resulted from a single imadazolone B (+142.03 Da) adduct on the lysine residue on the peptide $_{2186}$EITFP**K**MVANCCR$_{2198}$. A comprehensive listing of prominent consensus RyR2 peptides, the theoretical masses of the modification, and the AGEs involved are given in Table 2. We have also listed Schiff base and Amadori adducts (peptides with Δ masses of 162.02) that were detected because they are important intermediate products (last two rows of Table 2).

DISCUSSION

Decrease in cardiac contractility is one of the many complications that diabetic patients develop. However, this complication is of paramount importance because it contributes significantly to the increased incidence of morbidity and mortality in this patient group. Efficient cardiac contractions depend critically on the coordinated activity of several proteins involved in regulating/maintaining intracellular calcium homeostasis. One of these proteins is RyR2, the channel through which calcium ions leave the sarcoplasmic reticulum to trigger cardiac contraction. We and others have shown that expression of this protein decreases in hearts of chronic diabetic patients (8,9). Using the STZ-induced diabetic rat model, we have also shown that in addition to a decrease in expression, the functional integrity of RyR2 decreases with diabetes (14,15,19).

A principal finding of the present study is that RyR2 from 8-week STZ-induced diabetic rat hearts contains several non–cross-linking AGEs, including N^{ϵ}-(carboxymethyl)-lysine, imidazolone A, imidazone B, pyrraline, and AFGP. These post-translational products were detected by digesting RyR2 with trypsin, determining the masses of the resultant peptides using MALDI-TOF mass spectrometry and then searching the mass files for modifications using an in-house PERLscript program. These data are the first

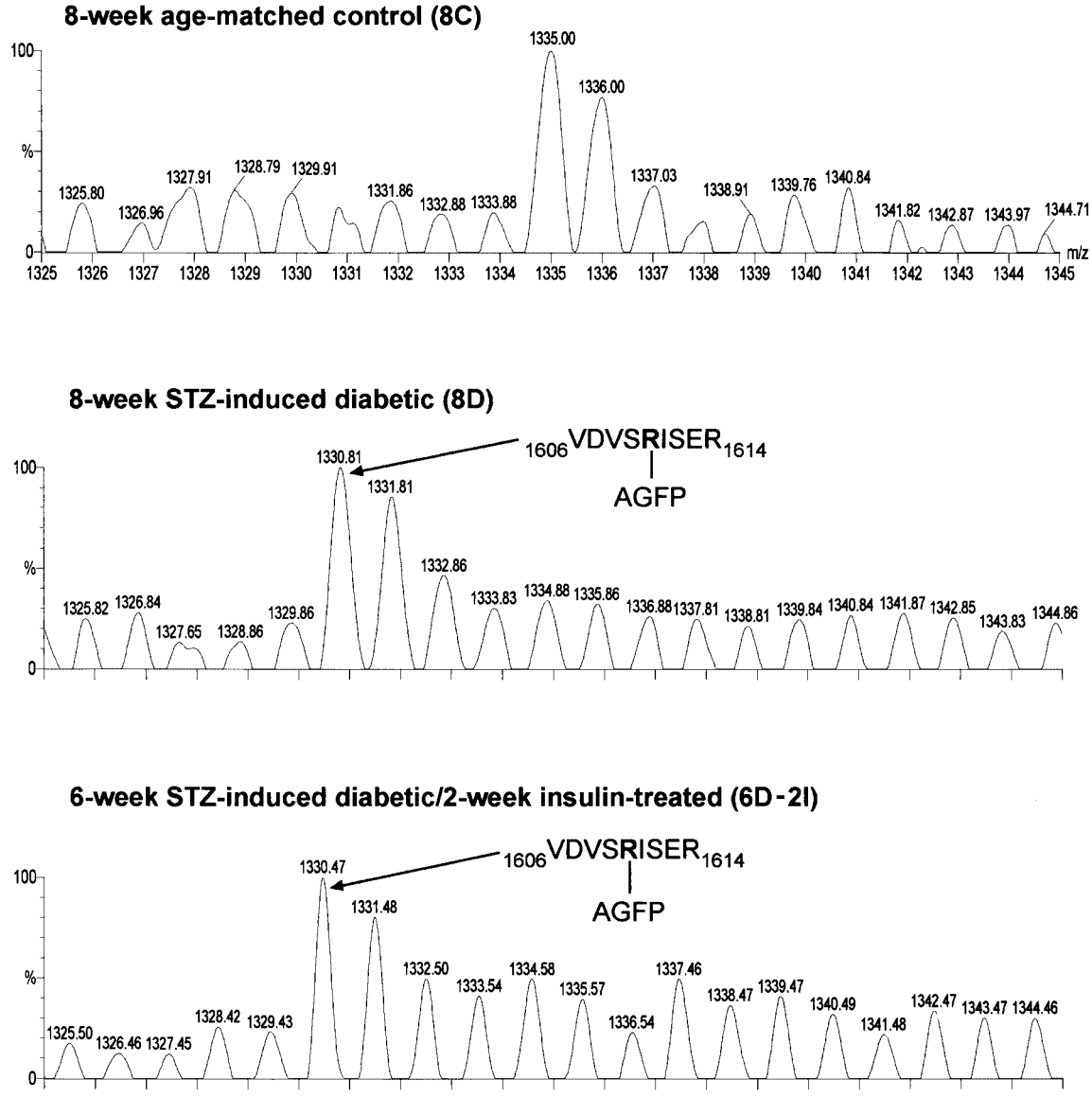

FIG. 8. Alignment of a select region of MALDI-TOF mass spectra obtained from trypsin digestion of RyR2 from 8C, 8D, and 6D-2I rat hearts. Spectra in the middle and lower panels show the prominence of $M+H^+$ peaks at 1330.81 Da for 8D and 1330.47 Da in 6D-2I. An equivalent signal is absent from 8C spectra. This peak is likely to result from an AFGP modification on arginine 1610, present on the miscleaved peptide $_{1606}$VDVSRISER$_{1614}$.

to show that AGEs are formed on intracellular RyR2 during chronic diabetes. This strategy also allowed us to determine not only the nature of the modifications but also the specific amino acids involved in the modifications.

In a previous study, we confirmed using a modified Langendorff procedure that hearts from 8-week STZ-induced diabetic rats show typical diabetic cardiomyopathic changes (15). In the present study, we show that the functional integrity of RyR2 from these hearts was compromised, as assessed from its decreased ability to bind [^{3}H]ryanodine, its altered sensitivity to calcium, and its slowed SDS-PAGE electrophoretic mobility. Taken together, these data suggest a relationship between a diabetes-induced decrease in activity of RyR2 and its AGE content. However, formation of AGEs on RyR2 is not the only contributor to its dysfunction and, by extension, the diabetic cardiomyopathy. In a previous study, we also showed that the dysfunction of RyR2 stems in part from a diabetes-induced increase in its disulfide bond content (19).

A second major finding of the present study is that non–cross-linking AGEs were also found on RyR2 from 6D-2I rat hearts. We also found that whereas insulin treatment was able to restore the calcium sensitivity of RyR2, RyR2 from 6D-2I bound 11.5% less [^{3}H]ryanodine per microgram of protein when compared with RyR2 from age-matched control animals (297.8 fmol [^{3}H]ryanodine/μg RyR2 compared with 336.6 fmol [^{3}H]ryanodine/μg RyR2). These data suggest that 2 weeks of insulin treatment, initiated after 6 weeks of diabetes was able to only partially prevent and/or reverse formation of these post-translation products on RyR2. Because the turnover rate of RyR2 is slow (~8 days [22]) and, once formed, AGEs remain chemically linked to the protein throughout its

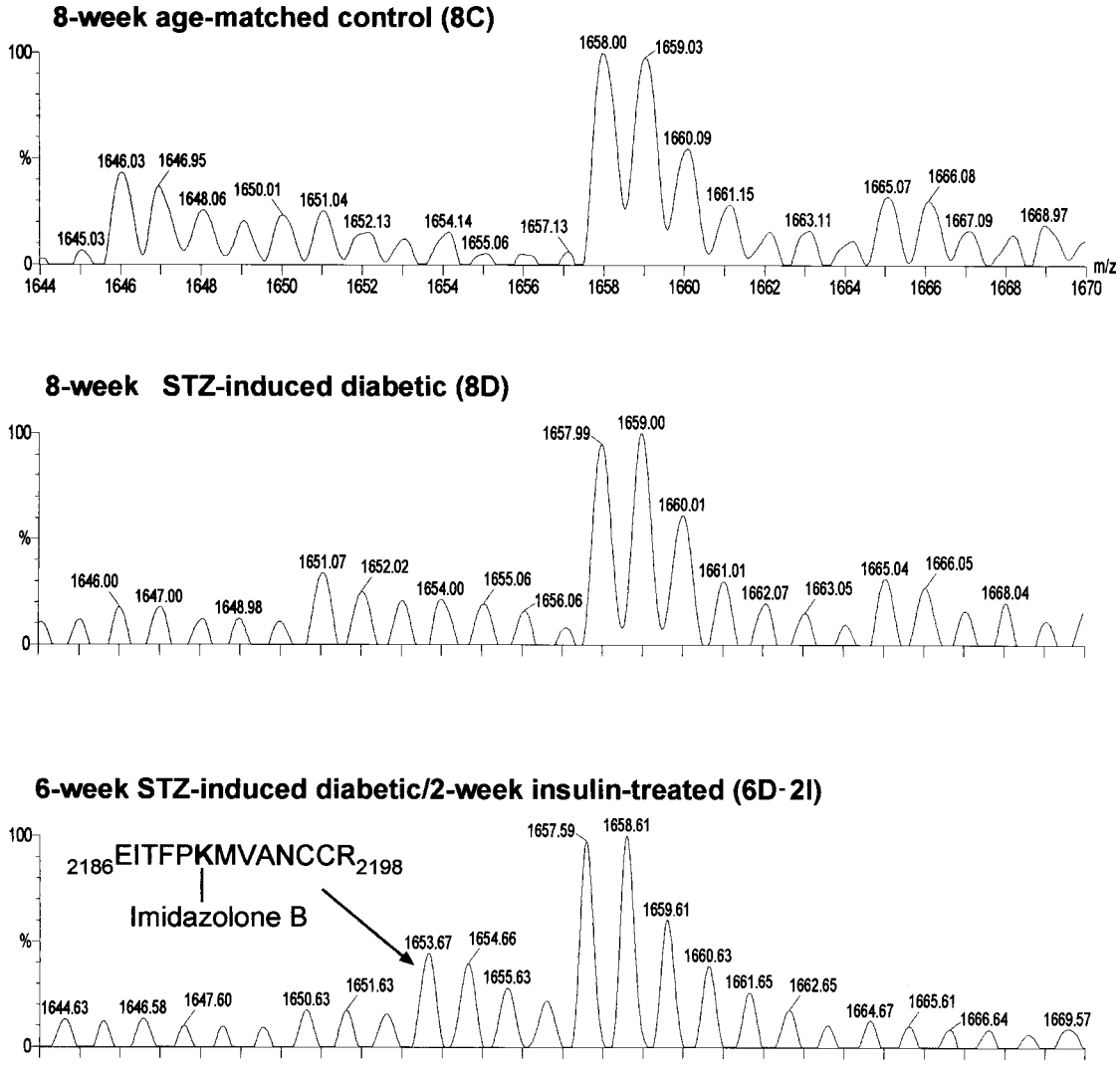

FIG. 9. Alignment of a select region of MALDI-TOF mass spectra obtained from trypsin digestion of RyR2 from 8C, 8D, and 6D-2I rat hearts. Spectrum in the lower panel shows the presence of an $M+H^+$ peak at 1653.67 Da on 6D-2I. The corresponding signal is absent from the spectra generated by RyR2 from 8C and 8D. This peak is likely to result from an imidazolone B modification on lysine 2191 present on the miscleaved peptide $_{2186}$EITFPKMVANCCR$_{2198}$.

lifetime, it is likely that the RyR2 analyzed may have consisted of a mixture of newly synthesized as well as not yet degraded AGE-modified RyR2.

In the present study, we also found that mRNA levels encoding RAGE as well its major spliced variant decreased after 8 weeks of diabetes. This result was surprising because we anticipated that mRNA levels for RAGE would increase after 8 weeks of diabetes. In a previous study, we found that membrane vesicles from 6-week STZ-induced diabetic rat hearts contain fluorophores with wavelength maxima (λ_{max}) were similar to those for AGEs (19). The latter suggested that in our STZ-induced diabetic rat model (50 mg/kg i.v. injected), AGEs may be formed on RyR2 as early as 6 weeks. If the latter holds true, then it is likely that the decrease in transcription of RAGE reflects receptor desensitization. Transcription of these proteins was restored to near control values with 2 weeks of insulin treatment, initiated after 6 weeks of diabetes.

In addition to these non–cross-linking AGEs, we also detected several RyR2 peptides from insulin-treated animals with Δ mass changes of 162.02 Da, consistent with modification by either a single Schiff base or an Amadori product. These data are clearly important because they also show for the first time the presence of AGE precursor molecules on RyR2. Although mass spectrometry is unable to differentiate between these two glycation products, this modification is more likely to have resulted from an Amadori product rather than a Schiff base. The latter is more labile and therefore likely degraded during the isolation and sample preparation procedures. Why these modifications were found in insulin-treated but not diabetic and control samples remains to be ascertained.

It is also of importance to note that the AGEs appeared to be found on "hot spots" on RyR2. Four modifications were detected between amino acids 1000–1700, three between amino acids 3400 and 3600, and three between amino acids 4400–4700 (Table 2). We speculate that because modifications are more likely to occur on regions of RyR2 that are exposed to higher concentrations of reducing sugars (i.e., the cytoplasmic side), then these "hot spots for glycation" are not likely to constitute the pore-forming and/or transmembrane segment of the chan-

TABLE 2
Peptides on RyR2 that are modified by glycation products

Peptide sequence	Theoretical mass ($M+H^+$) of peptide	Mass(es) ($M + H^+$) detected	Type of AGE modification on peptide (Δ mass)	Theoretical mass ($M+H^+$) of modified peptide	Mass(es) ($M+H^+$) detected
$_{4463}$LRQLTHTHR$_{4470}$	1060.61	1060.48 (c)	AFGP (270.07)	1330.68	
		1060.49 (d)			1330.81 (d)
		1060.46 (i)			1330.47 (i)
$_{1606}$VDVSRISER$_{1614}$	1060.57	1060.48 (c)	AFGP (270.07)	1330.68	
		1060.49 (d)			1330.81 (d)
		1060.46 (i)			1330.47 (i)
$_{3584}$KAVWHK$_{3590}$	768.44	1102.58 (c)	CML (58.02)	826.45	
		1102.58 (d)			826.13 (d)
		1102.47 (i)			826.14 (i)
$_{3598}$RAVVCFR$_{3605}$	921.51	921.41 (c)	Imidazolone A (144.03)	1065.57	
		921.41 (d)			
		921.52 (i)			1065.39 (i)
$_{1606}$VDVSRISER$_{1614}$	1060.57	1060.48 (c)	Imidazolone B (142.03)	1202.60	
		1060.49 (d)			1202.71 (d)
		1060.46 (i)			1202.47 (i)
$_{4463}$LRQLTHTHR$_{4470}$	1060.61	1060.48 (c)	Imidazolone B (142.03)	1202.63	
		1060.49 (d)			1202.71 (d)
		1060.46 (i)			1202.47 (i)
$_{3439}$MSKAAISDQER$_{3449}$	1235.60	1102.58 (c)	Imidazolone B (142.03)	1377.63	
		1102.58 (d)			1377.84 (d)
		1102.47 (i)			1377.50 (i)
$_{2186}$EITFPKMVANCCR$_{2198}$	1511.60	1511.80 (c)	Imidazolone B (142.03)	1653.75	
		1511.80 (d)			
		1511.72 (i)			1653.65 (i)
$_{2888}$EKAQDILK$_{2895}$	944.54	944.37 (c)	Pyralline (108.02)	1052.56	
		944.40 (d)			
		944.42 (i)			1052.41 (i)
$_{4677}$AALDFSDAREK$_{4687}$	1222.61	1222.59 (c)	Pyralline (108.02)	1330.63	
		1222.53 (d)			1330.81 (d)
		1222.46 (i)			1330.47 (i)
			Schiff base or Amadori product		
$_{1093}$TYAVKAGR$_{1100}$	865.48	865.59 (c)	(162.02)	1027.51	
		865.40 (d)			
		865.14 (i)			1027.21 (i)
			Schiff base or Amadori product		
$_{1349}$TAHGHLVPDR$_{1358}$	1102.57	1102.58 (c)	(162.02)	1264.59	
		1102.58 (d)			
		1102.47 (i)			1264.43 (i)

c, Control; d, diabetic sample; i, insulin-treated sample.

nel or reside within the lumen of the sarcoplasmic reticulum.

In conclusion, data from the present study suggest that loss in cardiac function induced by diabetes probably stems in part from a dysfunction of RyR2 (seen as a decrease in its ability to bind the specific ligand [^{3}H]ryanodine, alterations in its sensitivity to calcium, and a slowing in its electrophoretic mobility). In addition, this dysfunction could result from diabetes-induced formation of non–cross-linking AGEs on RyR2. Our data also show that 2 weeks of insulin treatment, initiated after 6 weeks of diabetes, only partially restored and/or prevented loss in RyR2 activity. Analysis of RyR2 from 6D-2I also showed that it contained several AGE adducts. Because RyR2 is a long-lived protein (~8 days) and AGE complexes remain on a protein throughout its lifetime, these data may help explain why congestive heart failure still persists in diabetic patients who are in compliance with insulin and/or oral hypoglycemic therapies.

ACKNOWLEDGMENTS

This work was supported by grants from the National Institutes of Health (HL66898) and Ralph W. and Grace R. Showalter Foundation.

REFERENCES

1. Rubler S, Dlugash J, Yuceoglu YZ, Kumral T, Branwood AW, Grishman A: New type of cardiomyopathy associated with diabetic glomerulo-sclerosis. *Am J Cardiol* 30:595–560, 1972
2. Hamby RI, Zoneraich S, Sherman S: Diabetic cardiomyopathy. *JAMA* 229:1749–1754, 1974
3. Asmal AC, Leary WP, Thandroyen FS: Diabetic heart disease. *Afr Med J* 57:788–790, 1980
4. Fein FS: Diabetic cardiomyopathy. *Diabetes Care* 13 (Suppl. 4):1169–1179, 1990
5. Bell DS: Diabetic cardiomyopathy: a unique entity or a complication of coronary artery disease? *Diabetes Care* 18:708–714, 1995
6. Janka HU: Increased cardiovascular morbidity and mortality in diabetes mellitus: identification of the high risk patient. *Diabetes Res Clin Pract* 30 (Suppl.):85–88, 1996

7. Bers DM: Cardiac excitation-contraction coupling. *Nature* 415:198–205, 2002
8. Guner S, Arioglu E, Tay A, Tasdelen A, Aslamaci S, Bidasee KR, Dincer UD: Diabetes alters mRNA levels of calcium-release channels in human atrial appendage (Abstract). *J Mol Cell Cardiol* 34(6):A84, 2002
9. Razeghi P, Young ME, Cockrill TC, Frazier OH, Taegtmeyer H: Downregulation of myocardial myocyte enhancer factor 2C and myocyte enhancer factor 2C-regulated gene expression in diabetic patients with nonischemic heart failure. *Circulation* 106:407–411, 2002
10. Yu Z, Tibbits GF, McNeill JH: Cellular functions of diabetic cardiomyocytes: contractility, rapid-cooling contracture, and ryanodine binding. *Am J Physiol* 266:H2082–H2089, 1994
11. Teshima Y, Takahashi N, Saikawa T, Hara M, Yasunaga S, Hidaka S, Sakata T: Diminished expression of sarcoplasmic reticulum Ca(2+)-ATPase and ryanodine sensitive Ca(2+) channel mRNA in streptozotocin-induced diabetic rat heart. *J Mol Cell Cardiol* 32:655–664, 2000
12. Netticadan T, Temsah RM, Kent A, Elimban V, Dhalla NS: Depressed levels of Ca^{2+}-cycling proteins may underlie sarcoplasmic reticulum dysfunction in the diabetic heart. *Diabetes* 50:2133–2138, 2001
13. Zhong Y, Ahmed S, Grupp IL, Matlib MA: Altered SR protein expression associated with contractile dysfunction in diabetic rat hearts. *Am J Physiol* 281:H1137–H1147, 2001
14. Bidasee KR, Dincer UD, Besch HR Jr: Ryanodine receptor dysfunction in hearts of streptozotocin-induced diabetic rats. *Mol Pharmacol* 60:1356–1364, 2001
15. Bidasee KR, Nallani K, Henry B, Dincer UD, Besch HR Jr: Chronic diabetes alters function and expression of ryanodine receptor calcium-release channels in rat hearts. *Mol Cell Biochem*. In press
16. Wolff SP, Jiang ZY, Hunt JV: Protein glycation and oxidative stress in diabetes mellitus and ageing. *Free Radic Biol Med* 10:339–352, 1991
17. Dhalla NS, Temsah RM, Netticadan T: Role of oxidative stress in cardiovascular diseases. *J Hypertens* 18:655–673, 2000
18. Evans JL, Goldfine RD, Maddux BA, Grodsky GM: Oxidative stress and stress-activated signaling pathways: a unifying hypothesis of type 2 diabetes. *Endocr Rev* 23:599–622, 2002
19. Bidasee KR, Nallani K, Besch HR Jr, Dincer UD: Streptozotocin-induced diabetes increased disulfide bond formation on cardiac ryanodine receptors (RyR2). *J Pharmacol Exp Ther*. Available at http://jpet.aspetjournals.org/cgi/reprint/jpet.102.046201v1.pdf.
20. Ulrich P, Cerami A: Protein glycation, diabetes, and aging. *Recent Prog Horm Res* 56:1–21, 2001
21. Baynes JW, Watkins NG, Fisher CI, Hull CJ, Patrick JS, Ahmed MU, Dunn JA, Thorpe SR: The Amadori product on protein: structure and reactions. *Prog Clin Biol Res* 304:43–67, 1989
22. Ferrington DA, Krainev AG, Bigelow DJ: Altered turnover of calcium regulatory proteins of the sarcoplasmic reticulum in aged skeletal muscle. *J Biol Chem* 273:5885–5891, 1998
23. Brownlee M, Cerami A, Vlassara H: Advanced glycosylation end products in tissues and the biochemical basis of diabetic complications. *N Engl J Med* 319:315–321, 1988
24. Bucala R, Cerami A: Advanced glycosylation, chemistry, biology and implications for diabetes and aging. *Adv Pharmacol* 23:1–34, 1992
25. Vasan S, Foiles PG, Founds HW: Therapeutic potential of AGE inhibitors and breakers of AGE protein cross-links. *Expert Opin Investig Drugs* 10:1977–1987, 2001
26. Soulis T, Thallas V, Youssef S, Gilbert RE, McWilliam BG, Murray-McIntosh RP, Cooper ME: Advanced glycation end products and their receptors co-localise in rat organs susceptible to diabetic microvascular injury. *Diabetologia* 40:619–628, 1997
27. Dincer UD, Bidasee KR, Guner S, Tay A, Ozcelikay AT, Altan VM: The effect of diabetes on expression of β_1-, β_2-, and β_3-adrenoreceptors in rat hearts. *Diabetes* 50:455–461, 2001
28. Lowry OH, Rosebrough NJ, Farr AL, Randall RJ: Protein measurement with the Folin phenol reagent. *J Biol Chem* 193:265–275, 1951
29. Cheng Y-C, Prusoff WH: Relationship between the inhibition constant (K1) and the concentration of inhibitor which causes 50 per cent inhibition (I50) of an enzymatic reaction. *Biochem Pharmacol* 22:3099–3108, 1973
30. Bidasee KR, Maxwell A, Reynolds WF, Patel V, Besch HR Jr: Tectoridins modulate skeletal and cardiac muscle sarcoplasmic reticulum calcium-release channels. *J Pharmacol Exp Ther* 293:1074–1083, 2000
31. Giron MD, Vargas AM, Suarez MD, Salto R: Sequencing of two alternatively spliced mRNAs corresponding to the extracellular domain of the rat receptor for advanced glycosylation end products (RAGE). *Biochem Biophys Res Commun* 251:230–234, 1998
32. Balshaw D, Gao L, Meissner G: Luminal loop of the ryanodine receptor: a pore-forming segment? *Proc Natl Acad Sci U S A* 96:3345–3347, 1999